PERFORMANCE CHARACTERISTICS OF A SPACE PLASMA SIMULATOR USING AN ELECTRON CYCLOTRON RESONANCE PLASMA ACCELERATOR AND ITS APPLICATIONS TO MATERIAL AND PLASMA INTERACTION RESEARCH

H. Tahara*, L. Zhang**, T. Yasui+ and T. Yoshikawa++

Faculty of Engineering Science, Osaka University

Toyonaka, Osaka, Japan

Abstract

A ground facility was developed for simulation of material and reactive space plasma interaction in LEO and for study of spacecraft charging and discharge phenomena. The space plasma simulator consisted of a vacuum tank 0.7 m in diameter × 1.5 m long, two turbo-molecular pumps with pumping speeds 5 and 3 m^3/s, respectively, achieving some 10^{-4} Pa, and an electron cyclotron resonance (ECR) plasma source of a magnetic-field-expansion plasma accelerator. Microwaves of maximum 500 W and 2.45 GHz were introduced into the discharge chamber of the plasma accelerator, and plasma generated by ECR heating was accelerated through a divergent magnetic field. The sample holder was located in oxygen or nitrogen plasma flows in the simulator. As a result, a clean low-pressure reactive-plasma environment could be produced with the plasma simulator. Plasma properties of plasma density, electron temperature, ion incident energy, ion freestream velocity and atomic oxygen flux were measured. The incident ion energy could be controlled by changing the sample holder potential. The ion freestream velocities for both gases had small variations for the sample holder potential. The flux of ions or atomic oxygens was large enough to simulate plasma environments around spacecrafts on ground for a shorter period than that in practical use in space. The simulator was found to have a high potential for ground material tests.

Introduction

Spacecrafts are in a severe environment in space. The surfaces of spacecrafts are exposed to energetic and reactive particles, such as electrons, ions, protons and oxygen atoms and ultraviolet light, during space missions. Furthermore, the electrostatic interactions between the surface materials and space plasmas, such as negative or positive sheath creation, and charging and arcing phenomena, frequently occur. In future long missions, materials in space will encounter a drastic decrease in performance of optical and/or electrical properties by bombardment of the particles and irradiation of high energy lights to their surfaces, and/or the surface materials may be destroyed by frequent electrical breakdown, i.e. arcing. Thus, the estimation of the decrease in performance of the physical properties is required in space before long use of materials, and also the mechanism of the material degradation, the structure of electrical sheaths and charging and arcing phenomena must be understood.

Space experiments on material degradation due to atomic oxygens or plasmas, on charging and discharge and on high voltage solar cells and plasma interactions, such as LDEF (Long Duration Exposure Facility), EOIM (Evaluation of Oxygen Interaction with Materials), SCATHA (Spacecraft Charging at High Altitude) and PIX (Plasma Interaction Experiment), were carried out by NASA etc in USA.[1-8] In Japan, flight experiments were initiated with the satellite ETS-V launched in 1987, and currently on ETS-VI and SFU (Space Flight Unit) many exposure experiments were conducted. On the other hand, ground facilities and computational codes also were developed to simulate the complex phenomena around spacecrafts on ground. In some ground simulations, spacecraft materials were exposed to energetic particles in vacuum chambers, in which the dose of each particle species was matched to a real condition in space.[9,10] In some experiments and computations, negative charging and arcing due to it, and high voltage solar array and plasma interactions were studied.[11-14] The energies of these charged particles ranged from several hundreds eV to a few keV, and physical phenomena caused by reactive charged particles with lower energies below 100 eV, such as charging and material degradation, are hardly simulated. One of the reason is that the development of a reactive particle accelerator realizing high flux and low energy was difficult.[15]

In Osaka University, a ground facility was developed to simulate plasma environments around spacecrafts, i.e. the physical and chemical interaction between materials and reactive space plasmas involving low energy charged particles, atomic oxygens and electric thruster plumes ; to investigate the electromagnetic or electrostatic interaction between electronic devices in satellites or high-voltage solar panels and the plasmas. In the present article, we reports operational characteristics of the space plasma simulator and plasma features generated in it.

Experimental Apparatus

The space plasma simulator, as shown in Fig.1, consists of a vacuum tank, vacuum pumps and a plasma accelerator. The electron cyclotron resonance (ECR) plasma accelerator is set on a flange of the large stainless vacuum tank 0.7 m in diameter × 1.5 m long. The main vacuum pumps are two oil-free turbo-molecular pumps

* Associate Professor, Member JSASS/AIAA
** Graduate Student of Osaka University
+ Research Associate, Member JSASS
++ Professor, Member JSASS/AIAA

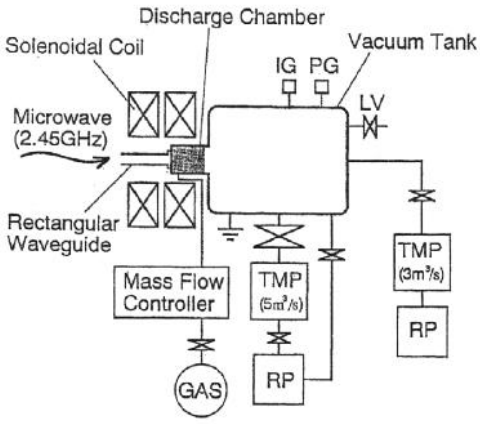

Fig.1 Schematic diagram of space plasma simulator with electron cyclotron resonance plasma accelerator.

(OSAKA VACUUM: TH5000VA and TH3000VA) with high pumping speed 5 and 3 m^3/s, respectively, each of which is connected to a rotary pump (ANELVA: T2033A). It takes about 90 minutes to achieve some 10^{-4} Pa of tank pressure using this pump system.

The ECR plasma accelerator, as shown in Fig.2, is a type of magnetic-field-expansion plasma accelerators.[16-19] Plasma is generated by ECR heating of the interaction between microwaves and divergent magnetic fields induced by a solenoidal coil around a discharge chamber and is electrostatically accelerated by micro electric fields induced by charge separation in the magnetic fields. Since the ECR plasma accelerator has negligible contamination because of no electrodes, clean and reactive plasma flows are expected to be generated in the space plasma simulator.[15] Microwaves of maximum 1 kW and 2.45 GHz are introduced into the discharge chamber 125 mm in inner diameter × 100 mm long across a quartz glass window 150 mm in diameter × 12 mm in width. As shown in Fig.2(b), there exists an ECR layer with 87.5 mT about 20 mm downstream from the quartz window at a solenoidal coil current of 95 A. Oxygen and nitrogen are used as working gases. After the mass flow rate is controlled with a commercially-available thermal-conductivity-type mass flow controller, the gas is radially injected from four ports just downstream of the quartz window into the discharge chamber.

Microwaves generated by a magnetron are transmitted in TE_{10} mode in a rectangular waveguide (WRJ-2(JIS): 109.2 × 54.6 mm) to the quartz glass window. The impedance of the transmission line is matched to that of a plasma load as closely as possible by an E-H tuner. Forward power (P_f) and reflected power (P_r) are measured with a directional coupler connected to a power monitor. Since the reflected powers were nearly zero for all experimental conditions, the absorbed powers ($P_i=P_f-P_r$) almost equaled the forward powers.

Ambient gas species in the vacuum tank are examined with a quadrupole mass spectrometer (BALZERS: QMG112). Plasma parameters of plasma density and electron temperature are measured with a Langmuir single probe, and incident ion energy is also measured with a three-grid electrostatic energy analyzer.[20-23]

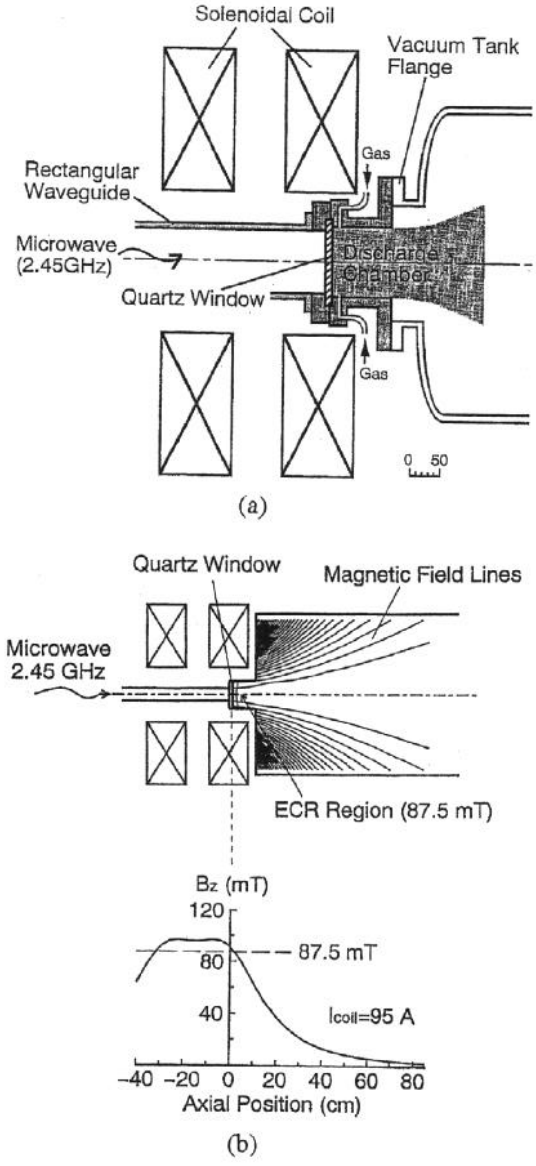

Fig.2 Cross section of electron cyclotron resonance plasma accelerator and calculated magnetic field lines and strength generated by solenoidal coils. (a) Cross section of electron cyclotron resonance plasma accelerator. (b) Calculated applied magnetic field lines and its strength on center axis.

Furthermore, a flux of oxygen atoms in a plasma is measured using a quartz-crystal microbalance (INFICON: QCM XTM/2) with a sensor surface coated with silver, and production of radicals in plasmas and energy excitations are examined by means of emission spectroscopy.[24]

Results and Discussion

Vacuum Environment

Figure 3 shows the typical mass spectra measured on a side wall about 800 mm downstream from the quartz glass window. Although the small output signal of N_2^+ is observed for no gas flow at an ambient gas pressure of 4.7×10^{-4} Pa after 90 minutes evacuation from an atmospheric environment, there exist many atomic and

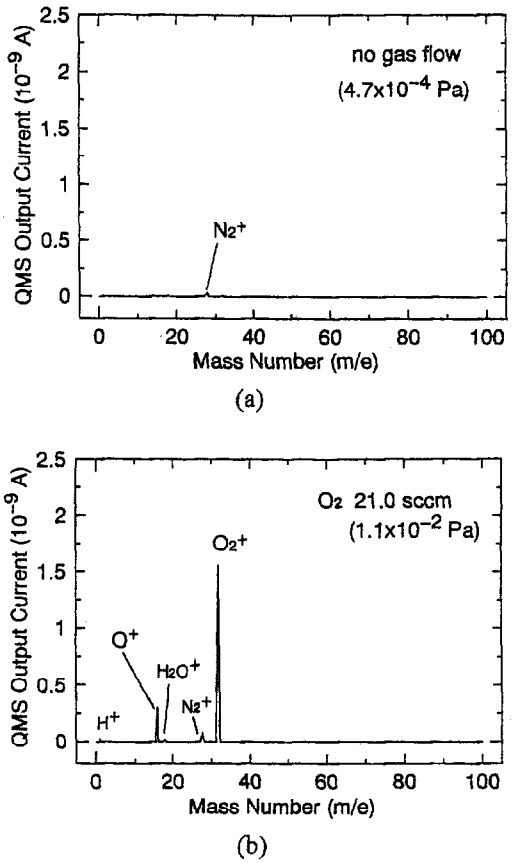

Fig.3 Typical mass spectra in space plasma simulator evacuated by 5-m³/s turbo-molecular pump. (a) Mass spectrum for no gas flow at ambient gas pressure of 4.7×10^{-4} Pa. (b) Mass spectrum for oxygen gas flow with flow rate of 21.0 sccm at 1.1×10^{-2} Pa.

molecular oxygens with an oxygen flow for no discharge. Since the signals of H_2O^+ and N_2^+ are very small and no carbonic species are observed, a clean low-pressure environment can be produced with the present pump system and even with the short pumping time.

Plasma Parameters

In order to determine the position of a sample holder, plasma parameters in plasma freestreams were measured. From their spatial profiles, the aluminous sample holder 100 mm in diameter × 3 mm thick, perpendicular to plasma flows, was determined to be located at an axial position of 700 mm downstream from the quartz glass window on the center axis of the ECR plasma accelerator and the vacuum tank. At the sample holder position, the mean free path was 300-500 m for electrons and about 50 m for ions. As a result, collisionless plasmas are created in the tank. The axial magnetic field strength was about 4 mT at the holder position, and the Rarmor radius for electrons was 2-3 mm. The Hall parameters for electrons and ions were orders of 10^5 and 10^3, respectively.

Figures 4 and 5 show the plasma parameters in front of the sample holder. They were measured with a cylindrical Langmuir probe axially located 20 mm upstream from the holder surface at a radial position of 25 mm from the center axis. The potential of the sample

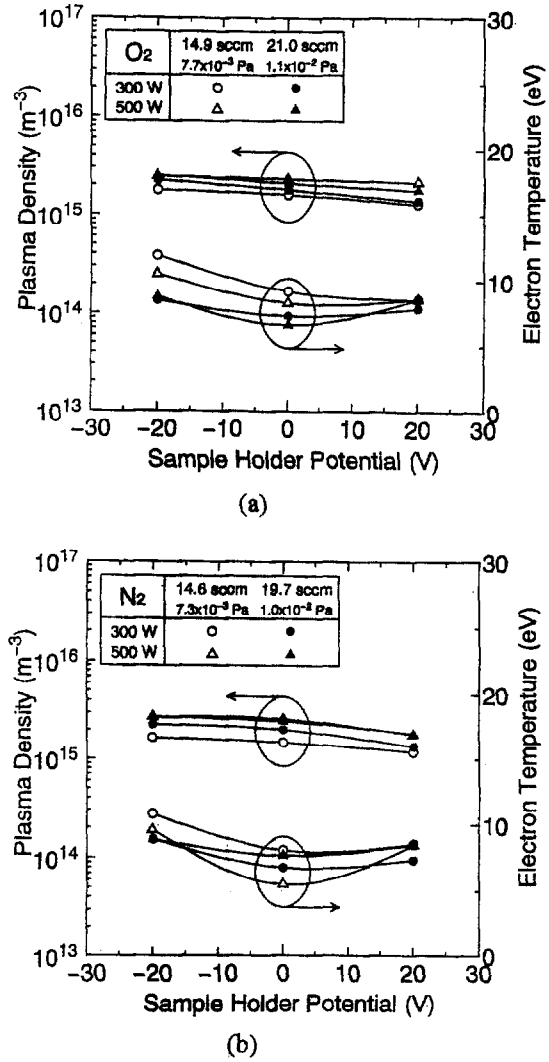

Fig.4 Plasma density and electron temperature vs sample holder potential characteristics for oxygen and nitrogen gases. (a) Oxygen gas. (b) Nitrogen gas.

holder was changed to -20, 0 and +20 V on ground potential of the vacuum tank potential. The plasma densities for oxygen and nitrogen gases slightly decrease with increasing sample holder potential, and they are 1.0-3.0×10^{15} m^{-3} above the order of 10^{11} m^{-3} of ion density in LEO. The plasma densities are slightly higher than those for no sample holder, i.e. in plasma freestreams, because of stagnation of plasma flows by the sample holder. On the other hand, the electron temperatures and the plasma space potentials for both gases are sensitive to the operational condition at low holder potentials of -20 and 0 V, and they range from 5 to 12 eV for the electron temperature and from 30 to 40 V for the plasma potential.

Incident Ion Energy, Ion Velocity and Ion Flux

Since spacecraft materials are considered to be intensively degraded by energetic ion bombardment, the ion energy into the sample holder were measured with variation of the holder potential. As shown with closed circles in Fig.6, the ion collector current of the energy analyzer, located at the same position of the Langmuir

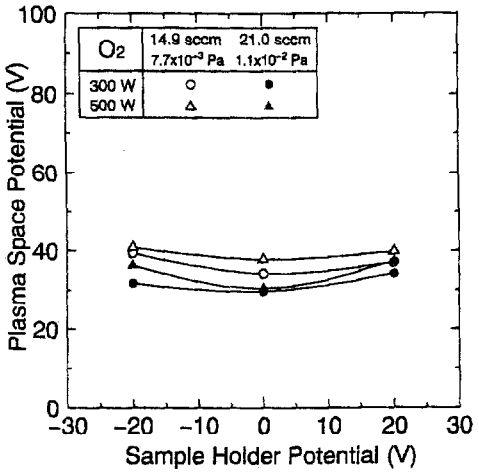

(a)

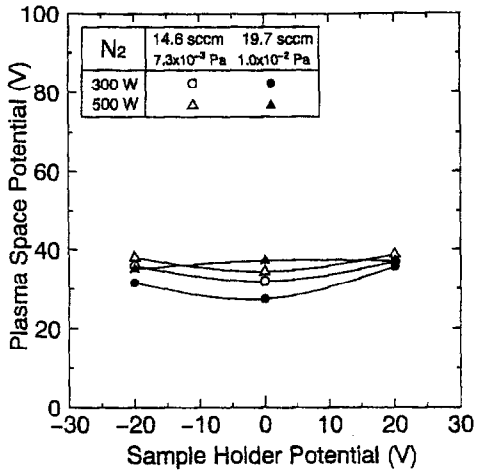

(b)

Fig.5 Plasma space potential vs sample holder potential characteristics for oxygen and nitrogen gases. (a) Oxygen gas. (b) Nitrogen gas.

probe, drastically decreases around the plasma space potential as shown in Fig.5(a) on the sample holder potential V_s-V_h (V_s: plasma space potential, V_h: holder potential), in which the ion reflecting voltage of a G_2 grid voltage on ground potential is varied.[20-23] Since the voltage V_s-V_h corresponds to the voltage of an ion sheath in front of the sample holder, ions in plasma freestreams are accelerated by this voltage just before attack to the sample holder. In other words, the holder surface is bombarded by ions with the sum of an energy corresponding to a freestream velocity and that corresponding to a sheath voltage. The derivative of the current signal, as represented with the solid line, has a peak at 45.0 V; that is, this energy corresponds to the mean incident ion energy, and the ion kinetic energy in a freestream is estimated to be the energy 15.2 V subtracting 29.8 V (=V_s-V_h) from 45.0 V. The half-value widths of peak characteristics of derivative lines became large with decreasing sample holder potential; i.e. the incident ion energy was widely distributed.

Figures 7 and 8 show the dependence of the incident ion energy, the ion flux and the ion freestream velocity on

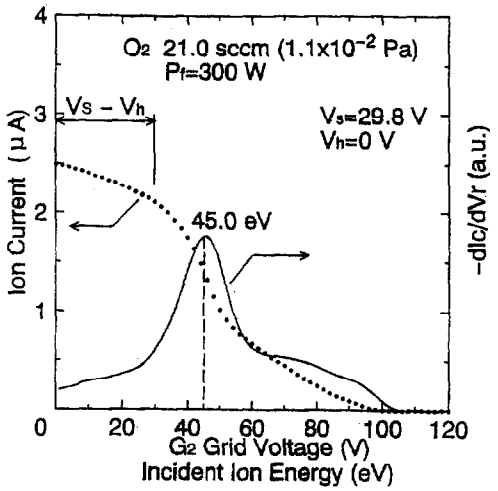

Fig.6 Typical ion collector current and its derivative of three-grids electrostatic ion energy analyzer. The closed circles represent the ion current I_c depending on the second-grid G_2 reflecting voltage V_r corresponding to the incident ion energy. The solid line represent the derivative $-dI_c/dV_r$ corresponding to the ion energy distribution function. The space plasma potential and the sample holder potential are represented with V_h and V_s, respectively.

the sample holder potential. The ion flux in the sample holder is estimated to be the plasma density shown in Fig.4 multiplied by the ion freestream velocity shown in Fig.8. The incident ion energies for both gases decrease linearly with an increase in the holder potential, and they range from 20 to 80 eV. The variation of the ion energy almost equals that of the holder potential. As a result, the incident ion energy can be controlled by changing the sample holder potential. Also, the ion energy is found to be larger at the lower flow rate or with the higher microwave power. As shown in Fig.8, the ion velocities for both gases have small variations for the sample holder potential, and it is 9-12 km/s for oxygen and 10-14 km/s for nitrogen. Accordingly, the existence of the sample holder hardly influences the ion velocity in a plasma flow generated by the ECR plasma accelerator although the plasma density and the plasma space potential are slightly changed with the sample holder. Also, the ion flux into the sample holder is relatively large, and it ranges from 1×10^{19} to 3×10^{19} ions/m^{2}sec for oxygen and from 1×10^{19} to 4×10^{19} ions/m^{2}sec for nitrogen. As a result, we can simulate the interaction between low energy ions and spacecraft materials with short operational periods on ground because of the large ion flux.

Atomic Oxygen Flux

The atomic oxygen flux into the sample holder was inferred using the silver-coated QCM, in which oxygen ions are reflected by applying a bias voltage above the plasma space potential to a grid in front of the sensor head.[24] When the silver coating on the sensor is oxygenated by oxygen atoms in a plasma flow, the natural frequency is changed by an increase in the sensor weight. Figure 9 shows the typical mass change vs exposure time characteristics. The drastic mass change around the start

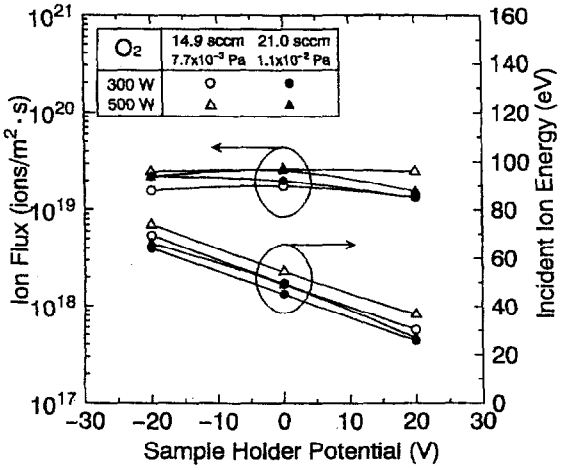

(a)

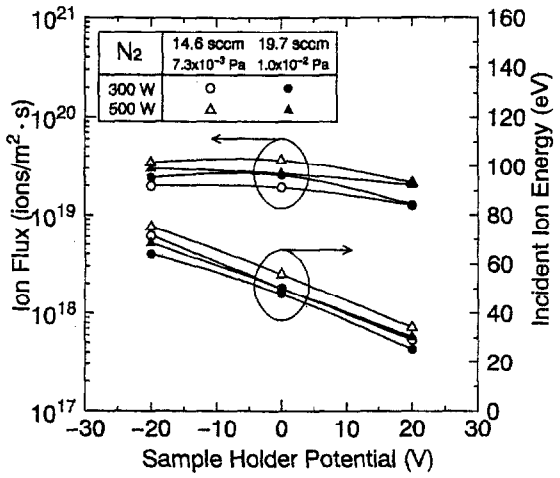

(b)

Fig.7 Dependence of sample holder potential on incident ion energy and ion flux into sample holder for oxygen and nitrogen gases. (a) Oxygen gas. (b) Nitrogen gas.

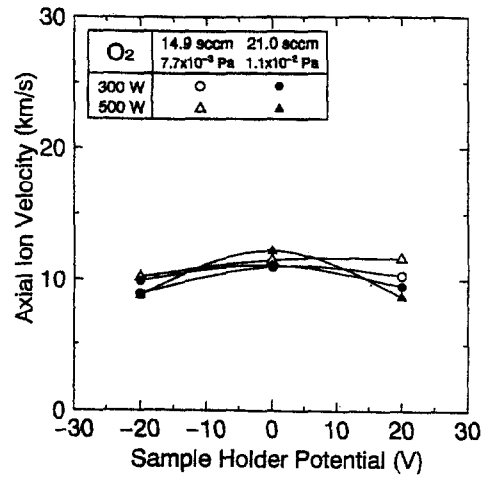

(a)

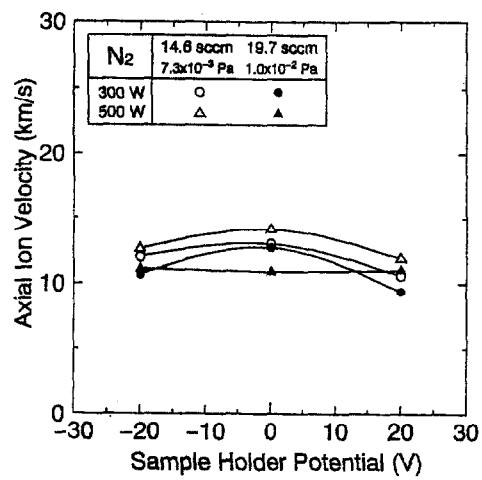

(b)

Fig.8 Ion freestream velocity vs sample holder potential characteristics for oxygen and nitrogen gases. (a) Oxygen gas. (b) Nitrogen gas.

of exposure shows oxygenation of the sensor surface. When the slope gradually decreases with the exposure time, oxygenation into the internal bulk, i.e. inner diffusion, is enhanced. We estimated the atomic oxygen flux from the slope at the start of exposure. The flux for an oxygen flow rate of 14.9 sccm is 7.91×10^{18} and 1.22×10^{19} atoms/m²sec at microwave powers of 300 and 500 W, respectively; for 21.0 sccm 9.50×10^{18} and 1.21×10^{19} atoms/m²sec at 300 and 500 W, respectively. An increase in the microwave power raises the atomic oxygen flux at a constant flow rate. The flux is an order of 10^{18}-10^{19} atoms/m²sec. Although the atomic oxygen flux is the same order as the ion flux, a much longer operational time will be required for ground simulation on atomic oxygen flow and materials interaction because of the larger oxygen atom density in LEO.

Plasma Emission Spectra and Exposure Tests

In the emission spectroscopic measurement, spectra of OI and OII for oxygen plasmas and of NII, N_2 and N_2^+ for nitrogen plasmas were mainly observed in front of the

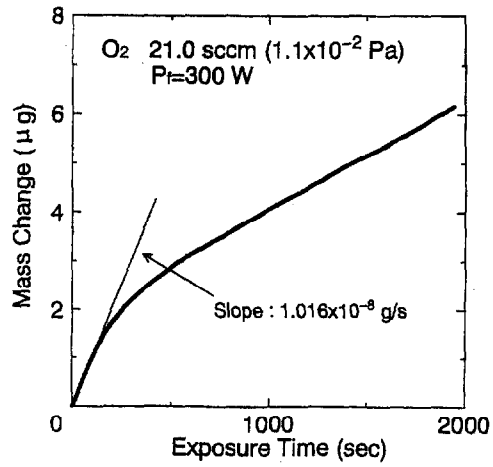

Fig.9 Typical dependence of exposure time on mass change of silver-coated sensor for quartz-crystal microbalance.

sample holder. Thus, energetic particles of many species were found to exist in the generated plasmas. Furthermore, preliminary tests of the interaction between Kapton films and oxygen plasma flows were carried out. X-ray photoelectron spectroscopic analysis showed that the addition reaction of oxygen atoms or the disruption or separation of various structural compounds occurred depending on incident ion energy and dose.

Conclusions

The ground facility was developed for simulation of material and reactive space plasma interaction in LEO and for study of spacecraft charging and discharge phenomena. The plasma simulator consisted of the vacuum tank 0.7 m in diameter × 1.5 m long, the two turbo molecular pumps with pumping speeds 5 and 3 m^3/s, respectively, achieving some 10^{-4} Pa, and the magnetic-field-expansion ECR-plasma accelerator. Microwaves of maximum 500 W and 2.45 GHz were introduced into the discharge chamber of the plasma accelerator, and plasma was generated by ECR heating of interaction between microwaves and the divergent magnetic field induced by the solenoidal coil outside the discharge chamber. The sample holder, biased from -20 to 20 V on ground potential, was located in oxygen or nitrogen plasma flows in the simulator. As a result, a clean low-pressure reactive-plasma environment could be produced with the plasma simulator. The plasma density in front of the sample holder was $1.0\text{-}3.0\times10^{15}$ m^{-3} above the order of 10^{11} m^{-3} of ion density in LEO. The incident ion energy into the sample holder ranged from 20 to 80 eV, and it could be controlled by changing the sample holder potential. The ion freestream velocities for both gases had small variations for the sample holder potential, and they were 9-12 and 10-14 km/s for oxygen and nitrogen, respectively. The ion flux into the sample holder ranged from 1×10^{19} to 4×10^{19} ions/m^2sec and the atomic oxygen flux from 7×10^{18} to 2×10^{19} atoms/m^2sec. These values were large enough to simulate plasma environments around spacecrafts on ground for a shorter period than that in practical use in space. Furthermore, preliminary tests of exposure of oxygen plasma flows to Kapton films were made, and the simulator was found to have a high potential for ground material tests.

References

1. Leger, L.J. and Visentine, J.T.," A Consideration of Atomic Oxygen Interactions with the Space Station," Journal of Spacecraft and Rockets, Vol.23, 1986, pp.505-511.
2. Synowicki, R.A., Hale, J.S., Spady, B., Reiser, M., Nafis, S. and Woollam, J.A.," Thin Film Materials Exposure to Low Earth Orbit Aboard Space Shuttle," Journal of Spacecraft and Rockets, Vol.32, 1995, pp.97-102.
3. Mcpherson, D.A. and Schober, W.R.," Spacecraft Charging at High Altitudes: The SCATHA Satellite Program," Progress in Astronautics and Aeronautics, Vol.47, 1976, pp.15-30.
4. Koons, H.C., Mizera, P.F., Roeder, J.L. and Fennell, J.F.," Severe Spacecraft-Charging Event on SCATHA in September 1982," Journal of Spacecraft and Rockets, Vol.25, 1988, pp.239-243.
5. Grier, N.T. and Stevens, N.J.," Plasma Interaction Experiment (PIX) Flight Results," NASA N79-24022, 1979, pp.295-314.
6. Ferguson, D.C.," The Voltage Threshold for Arcing for Solar Cells in LEO - Flight and Ground Test Results," NASA TM-87259, 1986.
7. Stevens, N.J.," Interactions between Large Space Power Systems and Low-Earth-Orbit Plasmas," NASA N85-22490, 1985, pp.263-276.
8. Stevens, N.J., Underwood, C.S. and Jones, M.R.,"Interpretation of High Voltage Solar Array Discharge Experiments," IEEE Transactions on Nuclear Science, Vol.37, 1990, pp.2120-2127.
9. Tahara, H., Zhang, L., Hiramatsu, M., Yasui, T., Yoshikawa, T., Setsuhara, Y. and Miyake, S.," Exposure of Space Material Insulators to Energetic Ions," Journal of Applied Physics, Vol.78, 1995, pp.3719-3723.
10. Zhang, L., Kawabata, T., Tahara, H., Yasui, T. and Yoshikawa, T.," Chemical Structural Changes and Optical Properties of Ion, Electron and Ultraviolet Light Irradiated Polyimide Films," 20th International Symposium on Space Technology and Science, Gifu, Paper 96-b-08, 1996.
11. Thiemann, H. and Bogus, K.P.," High Voltage Solar Cell Modules in Simulated Low-Earth-orbit Plasma," Journal of Spacecraft and Rockets, Vol.27, 1988, pp.278-285.
12. Kuninaka, H., Nozaki, Y., Satori, S. and Kuriki, K.," Ground Studies of Ionospheric Plasma Interactions with a High Voltage Solar Array," Journal of Spacecraft and Rockets, Vol.27, 1990, pp.417-424.
13. Kuninaka, H.," Space Experiment on Plasma Interaction Caused by High-Voltage Photovoltaic Power Generation," Journal of Spacecraft and Rockets, Vol.32, 1995, pp.894-898.
14. Hastings, D.E., Cho, M. and Kuninaka, H.," Arcing Rates for High Voltage Solar Arrays: Theory, Experiment, and Predictions," Journal of Spacecraft and Rockets, Vol.29, 1992, pp.538-554.
15. Tahara, H., Yasui, T., Onoe, K., Tsubakishita, Y. and Yoshikawa, T.," Microwave Ion Source Using Resonant Cavity," Japanese Journal of Applied Physics, Vol.32, 1993, pp.1298-1302.
16. Kaufman, D.A. and Goodwin, D.G.," Plume Characteristics of an ECR Plasma Thruster," Proceedings of the 23rd International Electric Propulsion Conference, Seattle, Vol.1, Paper IEPC-93-037, 1993, pp.355-360.
17. Hendel, H., Faith, T. and Hutter, E.C.," Plasma Acceleration by Electron Cyclotron Resonance," RCA Review, 1965, pp.200-216.
18. Miller, D.B. and Bethke, G.W.," Cyclotron Resonance Thruster Design Techniques," AIAA Journal, Vol.4, 1966, pp.835-840.
19. Kosmahl, H.G., Miller, D.B. and Bethke, G.W.," Plasma Acceleration with Microwaves near Cyclotron Resonance," Journal of Applied Physics, Vol.38, 1967, pp.4576-4582.
20. Hopwood, J., Reinhard, D.K. and Asmussen, J.," Charged Particle Densities and Energy Distributions in a Multipolar Electron Resonant Plasma Etching Source," Journal of Vacuum Science and Technology, Vol.A8, 1990, pp.3103-3112.

21. Oomori, T., Tuda, M., Ootera, H. and Ono, K.," Electrical and Optical Measurements of Electron Cyclotron Resonance Discharges in Cl_2 and Ar," Journal of Vacuum Science and Technology, Vol.A9, 1991, pp.722-726.
22. Reinke, P., Schelz, S., Jacob, W. and Moller, W.," Influence of a Direct Current Bias on the Energy of Ions from an Electron Cyclotron Resonance Plasma," Journal of Vacuum Science and Technology, Vol.A10, 1992, pp.434-438.
23. Charles, C.," Ion Energy Distribution Functions in a Multipole Confined Argon Plasma Diffusing from a 13.56-MHz Helicon Source," Journal of Vacuum Science and Technology, Vol.A11, 1993, pp.157-163.
24. Matijasevic, V., Garwin, E.L. and Hammond, R.H.," Atomic Oxygen Detection by a Silver-Coated Quartz Deposition Monitor," Review of Scientific Instrument, Vol.61, 1990, pp.1747-1749.